Obrabotka metallov (tekhnologiya, oborudovanie, instrumenty) = Metal Working and Material Science. 2021 vol. 23 no. 4 pp. 125–139
ISSN: 1994-6309 (print) / 2541-819X (online)
DOI: 10.17212/1994-6309-2021-23.4-125-139

NSTU NETI

Obrabotka metallov -
Metal Working and Material Science

Journal homepage: http://journals.nstu.ru/obrabotka_metallov

Enhanced assessment of technological factors for Ti-6Al-4V and Al-Cu-Mg strength properties

Kirill Zakharchenko [1, 2, a, *], *Vladimir Kapustin* [2, 1, b], *Alexey Larichkin* [1, 3, c]

[1] Lavrentyev Institute of Hydrodynamics SB RAS, 15 Ac. Lavrentieva ave., Novosibirsk, 630090, Russian Federation
[2] Novosibirsk State Technical University, 20 Prospekt K. Marksa, Novosibirsk, 630073, Russian Federation
[3] Novosibirsk State University, 1 Pirogova Str., Novosibirsk, 630090, Russian Federation

[a] https://orcid.org/0000-0003-2626-6184, zaharchenkok@mail.ru, [b] https://orcid.org/0000-0001-6124-2503, macler06@mail.ru,
[c] https://orcid.org/0000-0002-7306-9522, larichking@gmail.com

ARTICLE INFO

Article history:
Received: 04 August 2021
Revised: 16 September 2021
Accepted: 23 September 2021
Available online: 15 December 2021

Keywords:
Enhanced assessment
Cyclic loading
Elastoplastic strain
Strain characteristics
Dissipative characteristics
Finite element method

Funding
The reported study was funded by RFBR and Novosibirsk region according to the research project № 19-48-543028.

ABSTRACT

Introduction. The strength of construction materials when used under cyclic loads is of great importance in design engineering. A significant number of factors that affect the fatigue resistance have predetermined the creation of numerous methods that consider such influence. Nondestructive methods that are based on the connection of the physical degradation of material with strain properties enable evaluating experimentally the fatigue properties of materials. **Purpose of study**: the analysis of the processes of energy dissipation and strain accumulation during the inelastic cyclic strain of samples, using the *VT6* (*Ti-6Al-4V*) titanium alloy and the *D16* (*Al-Cu-Mg*) aluminum alloy before and after the technological impact. **The work experimentally investigates** the physical processes of degradation of the *VT6* and *D16* alloy samples that accompany the process of fatigue failure in materials with homogeneous and inhomogeneous stress-strain states in the concentrator (in the form of a hole and a weld). Typical modes are used to reach the fatigue testing that determine the critical stress in a material sample – the stress at which physical properties (temperature, strain) change without reaching the fatigue failure of samples. Critical stress amplitudes in the cycle, based on the data obtained during the experiment and the results of mathematical simulation, are compared. The effect of stress concentrators on critical loads that a detail can withstand after a unit operation is estimated by the finite-element method (*FEM*). **As a result**, the effect of the operational and technological factors on critical stress determined by strain and temperature is estimated. Comparative tests of the *VT6* and *D16* alloy samples with and without stress concentrators showed that the amplitudes of critical stress decrease by more than 30% in comparison with the ones that are without stress concentrators. The low-cycle fatigue tests of the *D16* alloy samples are carried out. Mathematical simulation of the cyclic strain of the samples is carried out using *MSC.Marc* package. The results of the cyclic loading tests, which show that the characteristics of the technological process reduce the amplitudes of the critical stress of the *VT6* and *D16* alloys and affect the fatigue properties of the *D16* aluminum alloy, **are discussed**. Mathematical simulation corresponded positively to the experimental data. Such correspondence indicates the possibility of conducting qualitative numerical assessments of the beginning of the inelastic strain accumulation process in structures with stress concentrators under the cyclic stress and the increasing stress amplitude, using the typical sample made of hardening elastoplastic material.

For citation: Zakharchenko K.V., Kapustin V.I., Larichkin A.Yu. Enhanced assessment of technological factors for Ti-6Al-4V and Al-Cu-Mg strength properties. *Obrabotka metallov (tekhnologiya, oborudovanie, instrumenty) = Metal Working and Material Science*, 2021, vol. 23, no. 4, pp. 125–139. DOI: 10.17212/1994-6309-2021-23.4-125-139. (In Russian).

Introduction

A large number of works [1] are devoted to methods for determining the characteristics of resistance, including the methods described in *GOST* 25.502-79. In enhanced methods of computational and experimental evaluation of the endurance limit of a material, several main groups can be conventionally distinguished.

*** Corresponding author**
Zakharchenko Kirill V., Ph.D. (Engineering), Associate Professor
Novosibirsk State Technical University,
20 Prospekt K. Marksa,
630073, Novosibirsk, Russian Federation
Tel.: 8 (383) 346-17-64, **e-mail:** zaharchenkok@mail.ru

The first group is the regular loading with fracture of samples at *LCF* (low-cycle fatigue) [2]. Coffin's formula is widely used, which includes the characteristic of inelastic deformation – the width of the hysteresis loop [3]. The second group of methods is loading using the effect of increasing the test frequency. This technique initiated the study of "infinite durability" – 10^6 – 10^{10} cycles (*Batias*) [4]. In this direction, researchers [5, 6] were the first to pay attention to the fact that under the loading regime of more than 10^9 cycles, cracks occur under the surface of the sample [7]. The fracture nucleus looks like a "Fish-eye" [8, 9]. In the third group, loading is considered using a programmed load change: *Lokati*, *Pro*, *Enomoto*, *Weibull* [10–12].

The general disadvantage of the three groups of enhanced methods considered above: destruction of a large number of samples, large error, it is realistic to evaluate only cyclically stable materials, which limits the presented methods. And also, the above methods are not associated with the study of physical processes that occur in the structure of the material at different scale levels, under the influence of external load.

The fourth group includes cyclic loading without bringing the samples to failure. In indirect methods, the value of the fatigue endurance limit is associated with the characteristics of the mechanical properties or physical phenomena of metals that accompany the fatigue process. These methods are based on establishing the relationship between fatigue limits and stresses at which irreversible effects associated with fatigue damage begin to appear in the test material. The physical basis of non-destructive methods is structurally sensitive characteristics and accompanying phenomena occurring in the material during cyclic loading [21-48]: phase transformations in the material [13-16], where transformations in alloys of the martensitic type are observed; microhardness [17], distortion of the crystal lattice of the metal [18], change in the characteristics of magnetic resistance, magnetic hysteresis, eddy currents [19-21], change in the surface relief [22, 23], acoustic emission [24], intensification of irreversible energy dissipation or inelastic deformations [22], changes in the microstructure [9, 23, 24], etc. There are methods in which the accumulation of damage is associated with a change in various integral characteristics of energy dissipation in the metal, based on the measurement of the absorption coefficient, the logarithmic decrement of oscillations, and the temperature in the fracture nucleus [25–30].

The main purpose of the study is to detect physical phenomena accompanying the process of cyclic loading in the transition region from elastic to inelastic deformation, analyze energy dissipation and accumulation of deformations that occur during inelastic cyclic deformation at constant non-zero average stresses. At the same time, the influence of technological impact on the determined characteristics is revealed. Further research is devoted to a discussion of approaches to these phenomena simulation.

Materials and Methods

Test samples

A batch of samples for study was made from a sheet of high-strength titanium alloy *VT6* (*Ti-6Al-4V*) and a sheet of aluminum alloy *D16* (*Al-Cu-Mg*). The choice of these materials is due to the fact that both alloys are widely used in aircraft construction. *D16* aluminum alloy has historically been the main material in the field of aircraft construction. Titanium alloy *VT6* is used, for example, for the manufacture of disks and blades of the first stages of gas turbine engines. These materials are supplied in various forms: forgings, stampings, rods, plates and sheets.

The history of the deformation of semi-finished products is created at the stage of its manufacture, in which a variety of technological processes affect the material: rolling, drawing, forging, machining, heat treatment, etc. Technological factors preceding the test of a material sample for fatigue failure resistance have a strong influence on the durability of the sample.

The study uses samples of type IV in accordance with *GOST* 25.502-79 (Fig. 1). The length of the working part of the sample is 50 and 45 mm, which makes it possible to install two extensometers for measuring axial and transverse deformations. Samples of *VT6* alloy were divided into two series: smooth

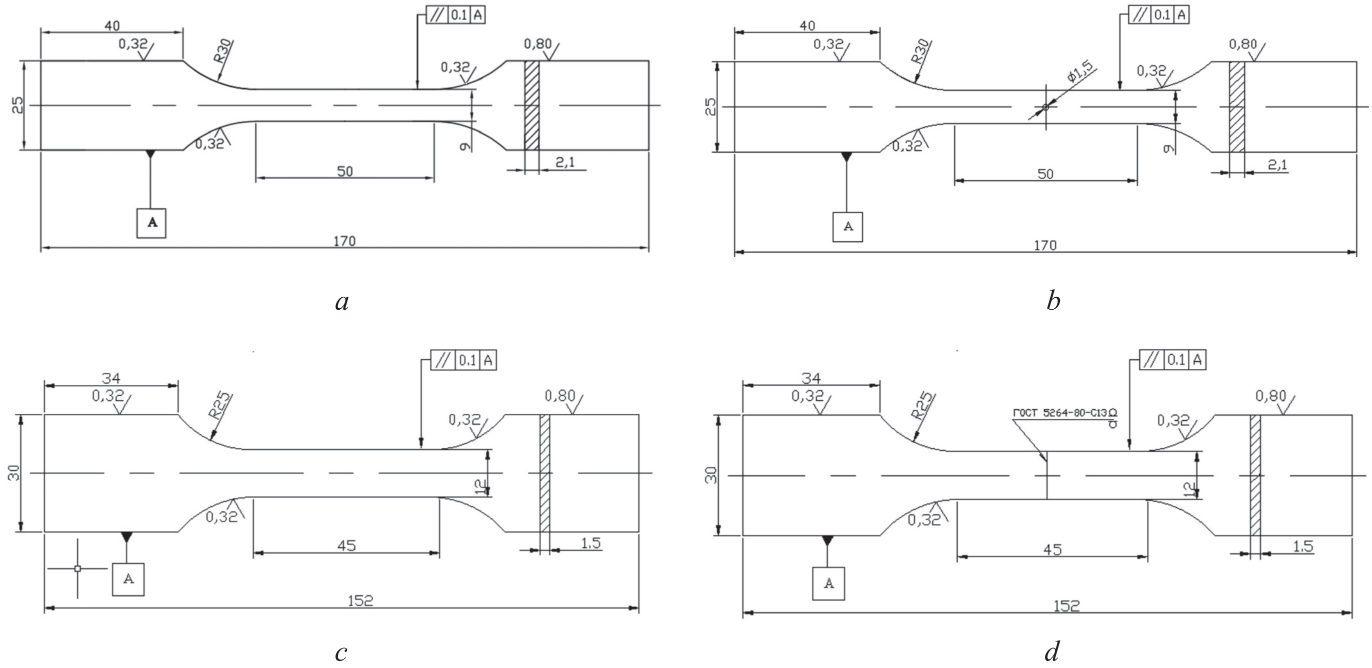

Fig. 1. Samples for testing

(Fig. 1, *a*) and with a stress concentrator in the form of a hole ($d = 1.5$ mm), in the center of the working part (Fig. 1, *b*). Samples had the following parameters: thickness ($h = 2.1$ mm), width ($b = 9$ mm), concentration factor $\alpha_\sigma = 6.49$. Specimens from alloy *D16* were also divided into two series: smooth (Fig. 1, c) and with a stress concentrator in the form of a weld (Fig. 1, d). Samples had the following parameters: thickness ($h = 1.5$ mm), width ($b = 12$ mm). The weld was formed using a laser. The width of the weld is equal to the thickness of the specimen. The strength of the weld was 0.85 of the strength of the base material.

The studies make it possible to assess the influence of design factors (stress concentrators) on the change in the characteristics of the state of the material under cyclic loading (as a result, on the resistance of the material to fatigue failure). Strain measurements were taken on a 25 mm base using an extensometer.

The stress-strain diagram for *VT6* and *D16* samples is shown in Fig. 2.

Mechanical properties of *VT6*:

– ultimate tensile strength $\sigma_u = 1045$ MPa (△),

– yield stress $\sigma_{0.2} = 881$ MPa (▲),

– modulus of elasticity $E = 102.600$ MPa.

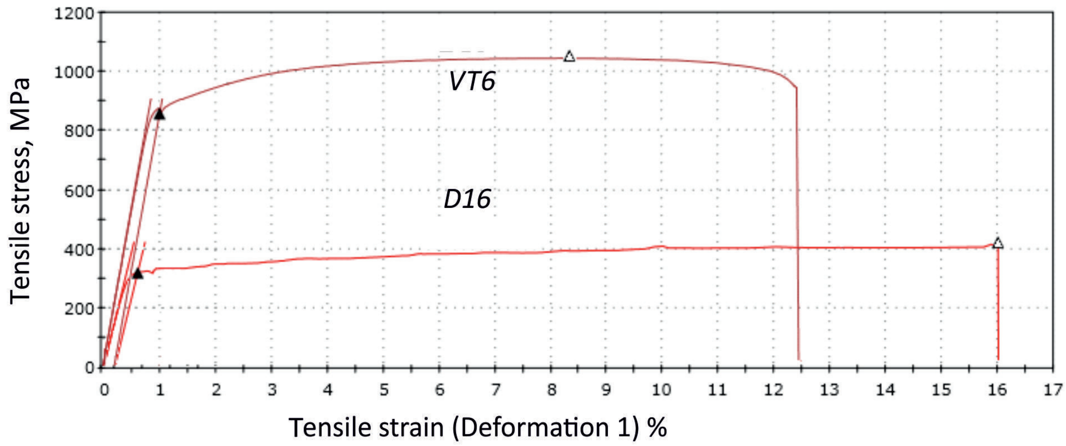

Fig. 2. Tensile stress diagrams for *VT6* and *D16* samples

Mechanical properties of *D16*

– ultimate tensile strength σ_u = 423 MPa (△),

– yield point $\sigma_{0.2}$ = 320 MPa (▲),

– modulus of elasticity E = 73.400 MPa.

The surface of the working part of the sample, intended for measuring the temperature with a thermal imager, was covered with a thin layer of amorphous carbon, which allows the emissivity to be brought closer to unity.

Experimental studies carried out with simultaneous measurement of two components of the strain tensor and the radiation temperature of the surface make it possible to provide completeness of data in solving problems of identifying material properties and in studying the processes of accumulation of irreversible deformations and energy dissipation by a sample.

Equipment

To load samples of *VT6* and *D16*, an *Instron* 8801 universal test system (England) was used. During testing, soft loading was implemented. To measure the increment of the total strain tensor components in situ, standard extensometers were used: "Dynamic Extensometer" No. 2620-601, "Transverse / Diametral Extensometer" No. W-E-404-F. The temperature was measured using an *ImageIR* "*InfraTec*" 8355 thermal imager with a temperature resolution of 0.02 K (Germany).

Method for determining the critical stress-strain state of a material under cyclic loading

In this work, it was required to determine the critical stress amplitude during cyclic loading of a material sample by changing the deformed state and dissipative heating.

For this purpose, a technique was used in which critical stresses can be determined using a diagram of the accumulation of irreversible deformations or by the temperature of dissipative heating of the material [26, 27, 32].

During the tests, the sample, which was in thermodynamic equilibrium, was subjected to soft loading with a certain constant average component of the stress cycle and a monotonically increasing stress amplitude, for example, increasing in proportion to time. Loading with a constant average component of the cycle made it possible to exclude the influence of the average stress and obtain the amplitude dependences of the characteristics of the deformed state and temperature on the stress amplitude.

A scheme of a typical loading program is shown in Fig. 3. It was a loading block consisting of 4 steps in which the following was performed:

– quasi-static deformation ("Step 1"),

– holding at this voltage for 180 sec ("Step 2"),

– soft loading with a step-like increase in the voltage amplitude ("Step 3"),

– unloading ("Step 4").

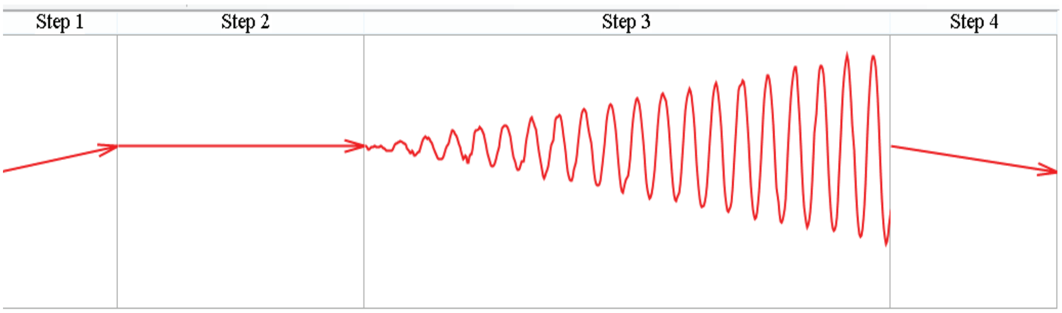

Fig. 3. A single loading block. "Step 1": quasi-static loading; "Step 2": holding under constant stress; "Step 3": harmonic cyclic loading with linearly increasing stress amplitude; "Step 4": unloading

"Step 3" contained 2.640 harmonic loading cycles at a frequency of 4 Hz for a total test duration of 660 seconds. holding at "Step 2" is necessary to establish thermodynamic equilibrium in the sample after its loading at "Step 1".

The magnitude of the load amplitude increment for each step $\sigma_{a\ step}$ was calculated by the formula: $\sigma_{a\ step} = \sigma_{a\ \max} / N_{cycle}$, where $\sigma_{a\_\max}$ is the maximum stress amplitude in "Step 3", N_{cycle} is the number of cycles in "Step 3". During the tests, the load, axial and transverse deformations, radiation temperature of the working surface of the sample were measured simultaneously. The tests were carried out at room temperature.

After completing the test program, the measurement data were analyzed and the extreme strain and temperature values were determined for each extreme stress in the test program.

The data obtained made it possible to isolate the components associated with irreversible deformation from the total deformations of the sample, as well as the parts associated with thermoelastic and dissipative heating of the sample from the temperature change, and determine the critical stress of the sample above which the process becomes irreversible.

Results and discussion

Stress-strain properties of the samples (alloys VT6 and D16) with and without a stress concentrator under cyclic loading

For samples made of *VT6* titanium alloy as delivered, Fig. 4 shows a comparison of the dependences of the increments of the average temperature values (ΔT_m) with the dependences of the stepping strain $\left(\varepsilon_{xm}^{p},\ \text{formula (1)}\right)$ on the stress amplitude (σ_a) (Fig. 4, *a*). Fig. 4, *b* shows a comparison of the dependences of the increments of the average temperature values (ΔT_m) with the amplitudes of irreversible longitudinal strain $\left(\varepsilon_{xm}^{p},\ \text{formula (2)}\right)$ on the stress amplitude (σ_a). Here:

$$\varepsilon_{xm}^{p} = \varepsilon_{xm} - \varepsilon_{xm0}\,, \tag{1}$$

$$\varepsilon_{xa}^{p} = \varepsilon_{xa} - \frac{\sigma_a}{E_{d0}}\,, \tag{2}$$

where $\varepsilon_{xm} = \dfrac{\varepsilon_{x\ \max} + \varepsilon_{x\ \min}}{2}$; $\varepsilon_{xa} = \dfrac{\varepsilon_{x\ \max} - \varepsilon_{x\ \min}}{2}$ – average and amplitude values of total longitudinal strain, $\varepsilon_{x\ \max}$, $\varepsilon_{x\ \min}$ – extreme values of longitudinal strain, ε_{xm0} total longitudinal strain after completion of "Step 2" of the loading program, σ_m; $E_{d0} = \dfrac{\sigma_a}{\varepsilon_{xa}}$ – secant dynamic modulus of elasticity, is calculated at the beginning of "Step 3", where inelastic deformations are insignificant.

Fig. 4 shows the dependences of the average temperature and the components of plastic strain on the stress amplitude. The numbers "1" and "2" denote the dependencies for samples with a hole and without a hole, respectively. The average stress was set to σ_m = 476 MPa and the maximum stress amplitude $\sigma_{a\ \max}$ = 529 MPa. If the experiments are performed for other average stresses, then it is possible to estimate the influence of the average stress in the loading cycle on the magnitude of the stress amplitude at which dissipative heating begins and the process of accumulation of inelastic strain is activated.

The presence of a concentrator in the sample in the form of a hole during periodic deformation with a constant average stress in a cycle decreases the value of the stress amplitude (σ_a) at which the process of plastic strain of the material is activated (Fig. 4, *a*); a nonlinear change in the average plastic axial strain and an increase in the average temperature of heating the sample are observed.

The presented diagram makes it possible to estimate the limit of cyclic elasticity of the *VT6* material (Fig. 4, *a*). Average values of irreversible plastic strain $\left(\varepsilon_{xm}^{p}\right)$ for samples with a hole and an increase in

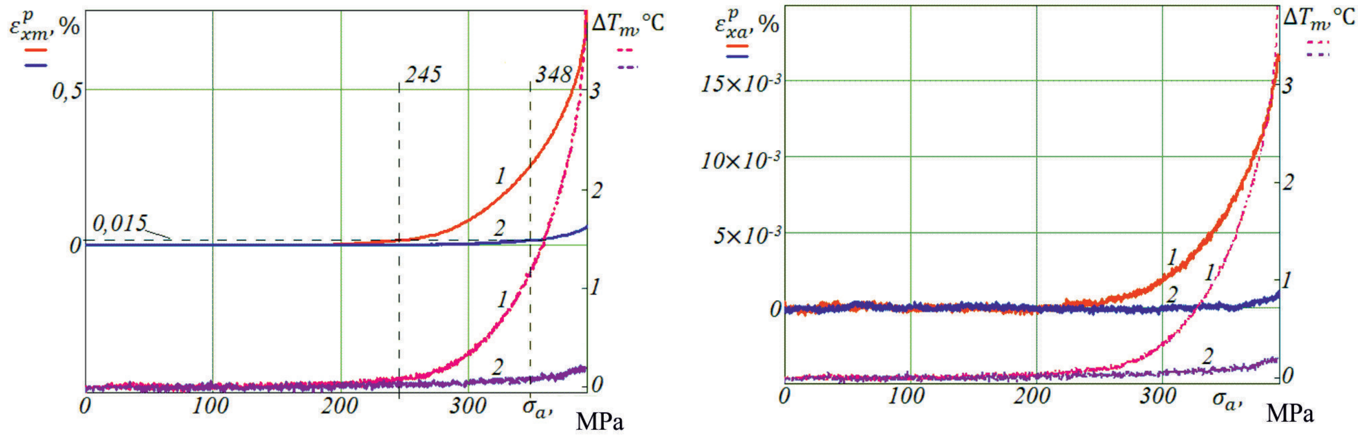

a *b*

Fig. 4. Evolution of parameters as a function of the stress amplitude for *VT6* (*Ti-6Al-4V*) samples with "1" and without a hole "2"; a) evolution of the temperature and the plastic mean axial strain; b) evolution of the temperature and the plastic axial strain amplitude

average temperature (ΔT_m) appear at a stress amplitude above 245 MPa, for smooth samples – at 348 MPa, respectively (with ε^p_{xm} = 0.015 %). This observation is consistent with the known softening effect of medium fatigue stress on metals, which is usually estimated from *Haigh* diagrams. At a stress amplitude of 348 MPa (Fig. 4, *a*), the average component of irreversible longitudinal strain $\left(\varepsilon^p_{xm}\right)$ and temperature increment (ΔT_m) are 16 and 10 times greater, respectively, for samples with a concentrator than for samples without a concentrator.

It can also be seen from (Fig. 4, *b*) that the presence of a concentrator for a sample made of *VT6* alloy leads to the fact that the amplitude of plastic axial strain has a higher value for a sample with a hole. When the stress amplitude (σ_a) is close to 400 MPa, the amplitude of irreversible strain $\left(\varepsilon^p_{xa}\right)$ increases by 0.017 % for samples with a stress concentrator.

The presence of a stress concentrator during periodic deformation of samples by a symmetric stress cycle with an average component leads to a decrease in the critical stress, at which irreversible processes are activated, by 30 %. This observation is consistent with the mathematical calculation presented in section «*Comparison of experimental data and results of mathematical simulation*».

To answer the question about the effect of the stress concentrator on dissipative heating and the average (amplitude) value of deformation in the cycle (stepping of the plastic hysteresis loop), a sample of *D16* aluminum alloy with and without a weld was loaded according to a similar program (Fig. 3) with an average stress in cycle (σ_m) and the maximum amplitude of the cycle stress ($\sigma_{a\ max}$) equal to 167 MPa.

Fig. 5 shows that in a sample of *D16* material with a stress concentrator (weld), an increase in the average plastic strain (stepping of the plastic hysteresis loop) and heating caused by plasticity occur much earlier than in smooth samples (without a stress concentrator). We remind that these results correspond to a fixed average stress σ_m = 167 MPa.

Thus, it can be seen from (Fig. 5, *a*) that for *D16* samples with a weld, the average values of irreversible plastic strain $\left(\varepsilon^p_{xm}\right)$ and the average temperature increment (ΔT_m) appear at a stress amplitude above 80 MPa, for smooth samples – at 130 MPa, respectively (with ε^p_{xm} = 0,02 %). The increase in the average and amplitude components of temperature occurs with a minimum discrepancy up to a stress amplitude of 100 MPa. At a stress amplitude of 130 MPa (Fig. 4, *a*), the average component of irreversible longitudinal deformation $\left(\varepsilon^p_{xm}\right)$ and temperature increments (ΔT_m) is 30 and 2 times higher, respectively, for samples with a weld than for samples without a weld.

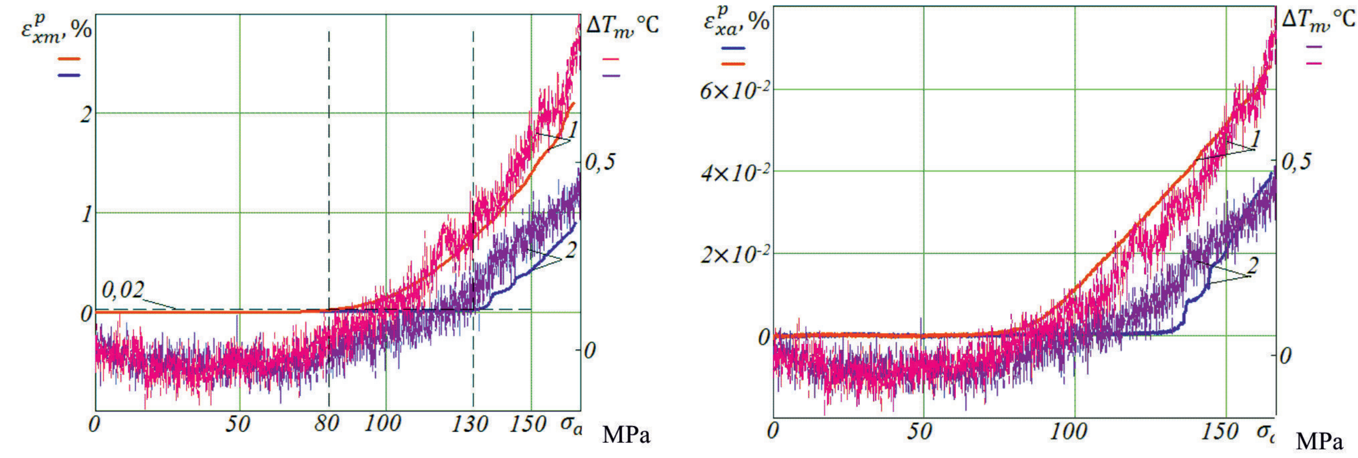

a *b*

Fig. 5. Evolution of parameters as a function of the stress amplitude for *D16* (*Al-Cu-Mg*) samples with "1" and without a weld "2"; a) evolution of the temperature and the average plastic axial strain; b) evolution of the temperature and the plastic axial strain amplitude

It can also be seen from (Fig. 5, *b*) that the weld in the alloy *D16* samples leads to the fact that the amplitude of the axial plastic strain has a higher value in the samples with a concentrator. When the stress amplitude (σ_a) is close to 160 MPa, the amplitude of irreversible deformations $\left(\varepsilon^p_{xm}\right)$ increases by 0.03 % for samples with a stress concentrator.

With periodic deformation of samples with a weld by a symmetric stress cycle with an average component, the critical stress decreases by 38 %.

For *D16* alloy samples, the kinetics of changes in the average plastic strain and average temperature during cycling at "Step 3" of the program (Fig. 3) with a constant amplitude of the stress cycle σ_a = 167 MPa was checked (Fig. 6).

For a smooth *D16* sample (Fig. 6, a), the average temperature increased monotonically during cycling (from ΔT_m = 0.4 °C to ΔT_m = 0.67 °C) at a constant stress amplitude σ_a = 167 MPa. In this case, the value

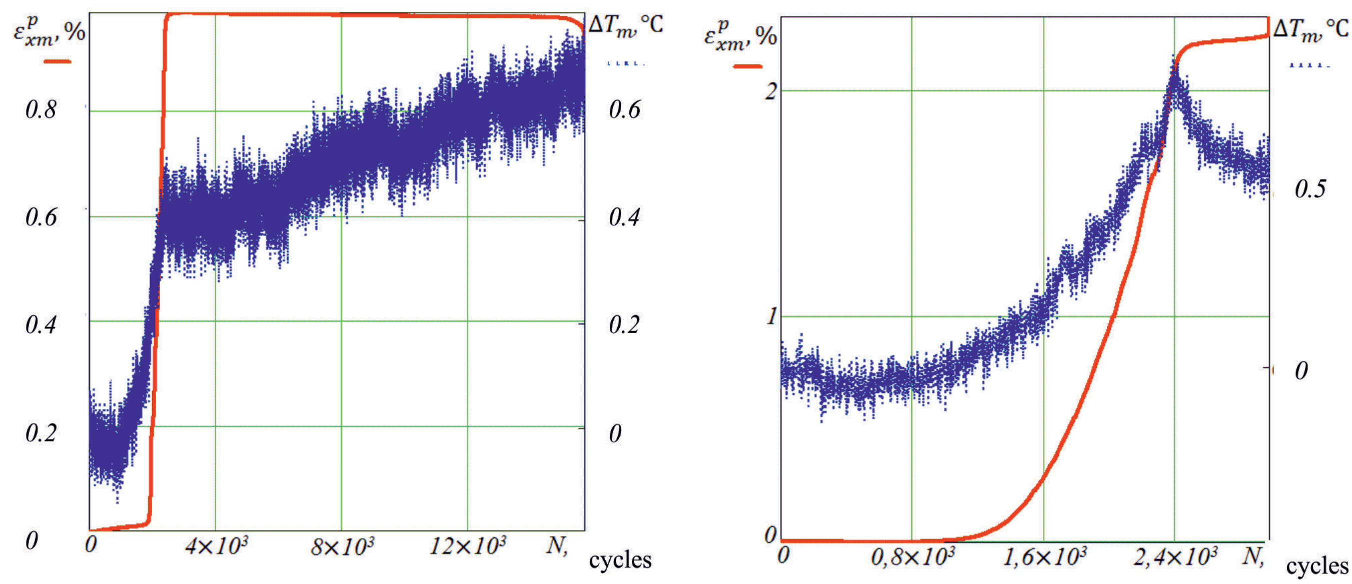

a *b*

Fig. 6. Evolution of the temperature and the plastic average axial strain versus the number of loading cycles for the samples a) *D16* (*Al-Cu-Mg*) without a weld; b) *D16* (*Al-Cu-Mg*) with a weld

of axial plastic strain remained constant $\varepsilon^p_{xm} \approx 1$ %. Whereas for the *D16* sample with a weld, the average temperature value decreased during cycling (from ΔT_m = 0.8 °C to ΔT_m = 0.55 °C) at a constant stress amplitude σ_a = 167 MPa. In this case, the value of axial plastic strain remained constant – more than $\varepsilon^p_{xm} \approx$ ≈ 2,2 %.

The average values of durability at the studied loading level of *D16* alloy are 2.9×10^3 and 15.7×10^3 cycles, respectively, for samples with and without a weld. Thus, a decrease in the characteristics of low-cycle fatigue for samples with a weld is obtained by more than 5 times. This shows the sensitivity of the method to the stress concentrator.

It can be assumed that during periodic asymmetric deformation of the sample beyond the elastic limit, two deformation effects are realized in the material.

The first effect is accompanied by an increase in the conventional yield stress (hardening) at which the accumulation of irreversible average strain is detected (the step of the plastic hysteresis loop). This effect is similar to material creep. The second effect is accompanied by a simultaneous increase in the amplitude of irreversible strain and an increase in the temperature of dissipative heating, which is accompanied by deterioration in strength properties. These effects require further research.

An increase in temperature and accumulation of average plastic strain has the same tendency: these processes begin at lower stress amplitudes for samples with a stress concentrator.

The results of experimental studies show the fundamental possibility of describing degradation processes under cyclic loading. The method will also allow assessing the influence of technological influences to which the sample of the material was previously subjected. The method can be used as an alternative to the destructive methods of testing structures for strength and assessing the characteristics of resistance to fatigue fracture of metallic materials.

Comparison of experimental data and results of mathematical simulation

The results of finite element modeling (*FEM*) of cyclic stretching of a strip of *VT6* with a hole and a strip without a hole, as well as a strip of *D16* with a weld and a strip without a weld are compared. The models were a quarter of a sample with a measurement base of L_0 = 12.5 mm. Symmetry conditions were set on surfaces coinciding with the coordinate planes O_{xz} and *Oyz*. A load was applied to the upper surface of the samples, the history of which corresponded to that in the experiment. The values of the elasticity and plasticity parameters of the material were assumed to correspond to the *VT6* and *D16* alloys, respectively. The weld material for the *D16* sample was assumed to be the same as for the base material, but with a reduced yield stress and strength equal to 0.85 of $\sigma_{0.2}$ and σ_u. The limiting deformation of the weld material was assumed to be equal to 1.15 of the limit for the base material *D16* (see Fig.2). The calculated deformed configurations and the values of the intensity of total strain for samples from the alloys under consideration are shown in (Fig. 7).

Fig. 8 shows the diagrams of the dependence of the average component of the strain of the sample measurement base in the cycle on the stress amplitude in the cycle of a flat sample with a hole from *VT6* (Fig. 8, *a*) and for a flat sample with a weld after laser welding (Fig. 8, *b*). Lines *1* correspond to the data of simulation the cyclic deformation of flat samples with stress concentrators (a hole for a *VT6* samples and a weld for *D16* samples), lines 2 denote data for samples of the corresponding dimensions, for each alloy, without stress concentrators.

It can be noted that the voltage amplitudes correspond satisfactorily between the experimental values and the results of mathematical simulation. At these stress amplitudes, irreversible accumulation of strain of the sample occurs on the measurements base of 25 mm. Data on sample sizes and stress amplitudes are given in Table.

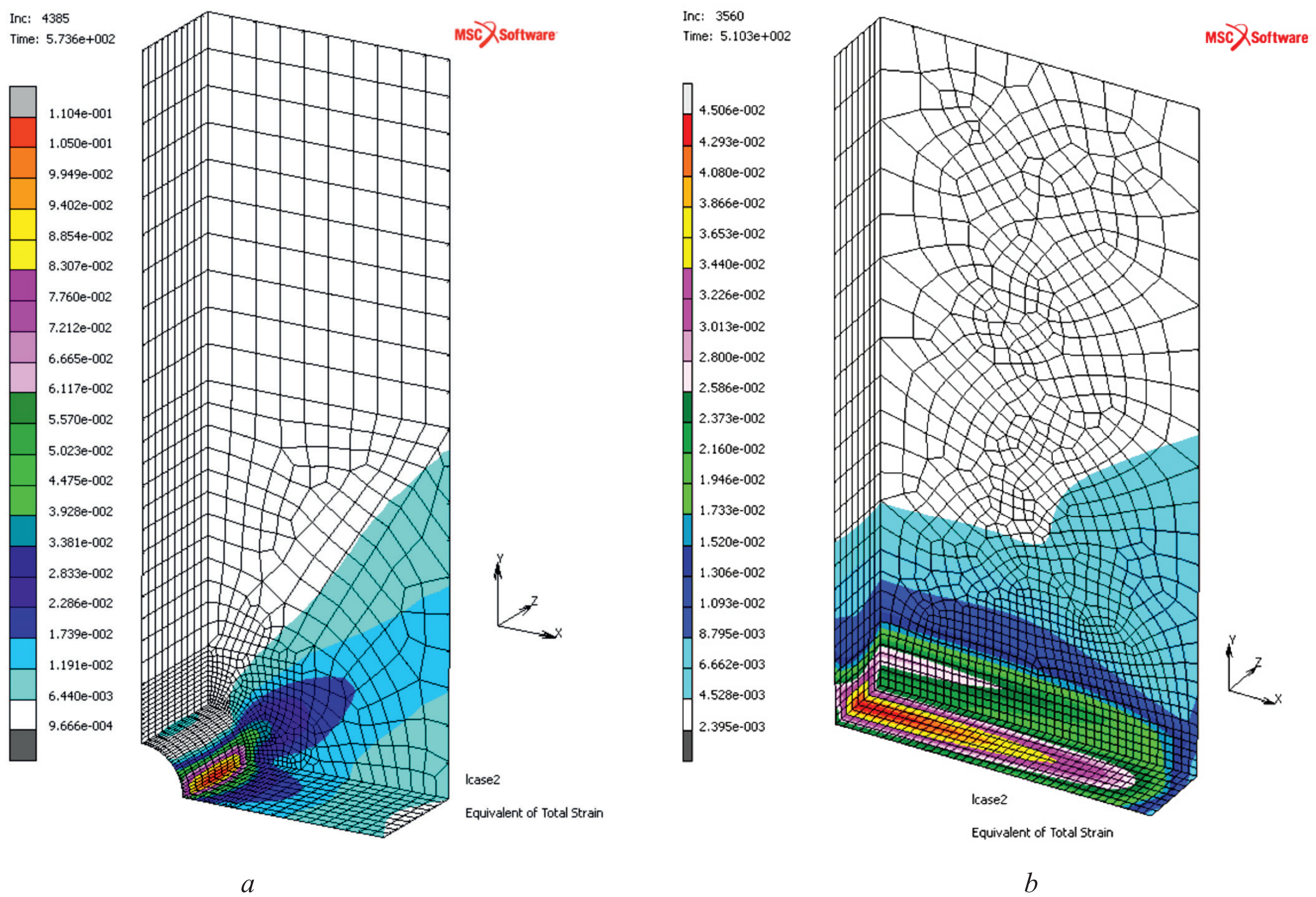

Fig. 7. Distribution of total strain intensity for samples:
a – from VT6 (Ti-6Al-4V) alloy with a hole; *б* – from D16 (Al-Cu-Mg) alloy with a laser weld

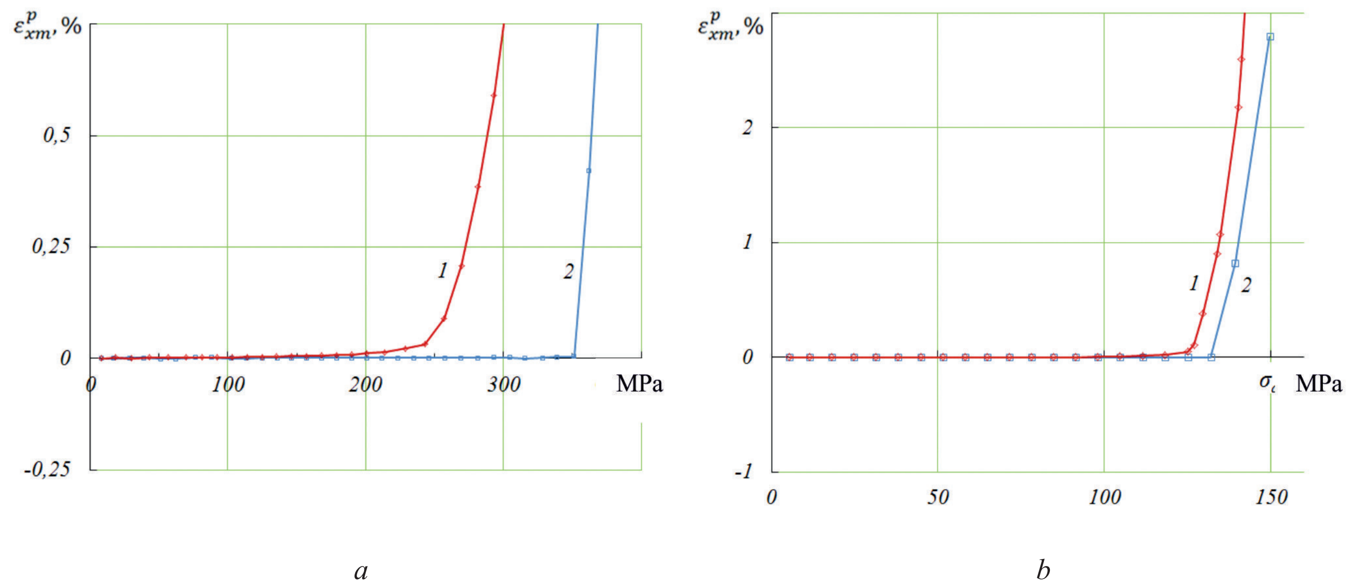

Fig. 8. Evolution of the average plastic axial strain as a function of the stress amplitude for samples: a) made of *VT6* (*Ti-6Al-4V*) alloy with hole “1” and without it “2” b) made of alloy *D16* (*Al-Cu-Mg*) with weld “1” and without it “2”

Sample data and comparison of simulation and experiment results

Sample material	Sample type	Sample dimensions		Stress concentrator dimensions, mm	Stress Amplitude in the experiment $\sigma_a^{\exp}$, MPa	Stress amplitude in simulation σ_a^{num}, MPa
		h, mm	*b*, mm			
VT6 /(*Ti-6Al-4V*)	without a hole	2.1	9	–	348	351
	with a hole			Ø1.5	245	223
D16 / (*Al-Cu-Mg*)	without a weld	1.5	12	–	130	132
	without a weld			□1.5	80	118

Conclusions

1. Experimental dependences of temperature and total strains on the magnitude of the stress amplitude are obtained for homogeneous and inhomogeneous stress-strain state in the region of concentrators, which simulate the influence of technological factors on the strength of samples made of titanium (*VT6*) and aluminum (*D16*) alloys.

2. It is established that:

a) the amplitude of critical stresses for samples made of *VT6* alloy with a stress concentrator in the form of a hole is less by 30 % or more than that of samples without holes;

b) the amplitude of critical stresses of samples made of alloy *D16* with a concentrator in the form of a weld is 38 % less than that of samples without weld.

3. Verification fatigue tests of the samples confirmed the validity of the accelerated assessments and conclusions 2.

4. The simulation results for flat samples with a hole and with a weld showed satisfactory agreement of the stress amplitudes between the experimental data and the simulation results. This correspondence makes it possible to carry out qualitative numerical estimates of the onset of accumulation of inelastic strain in structures with stress concentrators during cyclic deformation with an increasing stress amplitude. The modeling used a standard model of an elastoplastic body with hardening.

References

1. Troshchenko V.T., Sosnovskii L.A. *Soprotivlenie ustalosti metallov i splavov* [Fatigue resistance of metals and alloys]. Kiev, Naukova Dumka Publ., 1987. 1302 p.

2. Ivanova V.S. Strukturno-energeticheskaya teoriya ustalosti metallov [Structural-energy theory of fatigue of metals]. *Tsiklicheskaya prochnost' metallov* [Cyclic strength of metals]. Moscow, Academy of Sciences of the Soviet Union Publ., 1962, pp. 11–23.

3. Coffin L.F. Low-cycle fatigue: a review. *Applied Material Research*, 1962, vol. 1, no. 3, pp. 129–141.

4. Bathias C. *Gigacycle fatigue in mechanical practice*. Vergal, Marcel Dekker, 2005. 304 p. ISBN 9780203020609. DOI: 10.1201/9780203020609.

5. Naito T., Ueda H., Kihushi M. Fatigue behavior of carburized steel with internal oxides and non-martensitic microstructure near the surface. *Metallurgical Transactions A, Physical Metallurgy and Materials Science*, 1984, vol. 15, no. 7, pp. 1431–1436.

6. Kanazawa K., Nishijima S. Fatigue fracture of low alloy steel at ultra-high cycle regime under elevated temperature conditions. *Journal of the Society of Materials Science*, 1997, vol. 46, no. 12, pp. 1396–1400. DOI: 10.2472/jsms.46.1396.

7. Murakami Y., Nomoto T., Ueda T. Factors influencing the mechanism of superlong fatigue in steels. *Fatigue and Fracture of Engineering Materials and Structures*, 1999, vol. 22, no. 7, pp. 581–590. DOI: 10.1046/j.1460-2695.1999.00187.x.

8. Shiozawa K., Nashino S., Morii Y. Subsurface crack initiation and propagation mechanism of high-strength steelin very high cycle fatigue regime. *International Journal of Fatigue*, 2006, vol. 28, no. 11, pp. 1521–1532. DOI: 10.1016/j.ijfatigue.2005.08.015.

9. Shanyavskii A.A. *Modelirovanie ustalostnykh razrushenii metallov: sinergetika v aviatsii* [Modeling of fatigue cracking of metals. Synergetics for aviation]. Ufa, Monografiya Publ., 2007. 500 p. ISBN 978-5-94920-058-2.

10. Locati L. Le prove di cafica come ausilio alla prodetta sone ed alle predusioni. *Metallurgia Italiana*, 1955, vol. 47, no. 9, pp. 245–260.

11. Prot E.M. Une nouvelle technique d'essai des materiaux. L'essai de fatigue sous chrse progressive. *Revue de Metallurgie*, 1948, vol. 45, no. 12, pp. 481–496.

12. Enomoto N. A method for determining the fatigue limit of metals by means of stepwise load increase tests. *Proceedings – American Society for Testing and Materials*, 1959, vol. 59, pp. 711–722.

13. Glage A., Weidner A., Biermann H. Effect of austenite stability on the low cycle fatigue behaviour and microstructure of high alloyed metastable austenitic cast TRIP-steels. *Procedia Engineering*, 2010, vol. 2, no. 1, pp. 2085–2094. DOI: 10.1016/j.proeng.2010.03.224.

14. Terent'ev V.F., Dobatkin S.V., Prosvirnin D.V., Bannykh I.O., Rybal'chenko O.V., Raab G.I. Ustalostnaya prochnost' austenitnoi stali Kh18N10T posle ravnokanal'nogo uglovogo pressovaniya [Fatigue strength of austenitic steel of Kh18N10T grade after equal-channel angular extrusion]. *Deformatsiya i razrushenie materialov = Russian Metallurgy (Metally)*, 2008, no. 10, pp. 30–38. (In Russian).

15. Yang Y.S., Bae J.G., Park C.G. Improvement of the bending fatigue resistance of the hyper-eutectoid steel wires used for tire cords by a post-processing annealing. *Materials Science and Engineering: A*, 2008, vol. 488, no. 1–2, pp. 554–561. DOI: 10.1016/j.msea.2007.11.048.

16. Makarov A.V., Savrai R.A., Schastlivtsev V.M., Tabatchikova T.I., Yakovleva I.L., Egorova L.Y. Structural features of the behavior of a high-carbon pearlitic steel upon cyclic loading. *The Physics of Metals and Metallography*, 2011, vol. 111, no. 1, pp. 95–109. DOI: 10.1134/S0031918X11010091. Translated from *Fizika metallov i metallovedenie*, 2011, vol. 111, no. 1, pp. 97–111.

17. Shchipachev A.M., Poyarkova E.V. Vliyanie ustalostnoi povrezhdaemosti na tverdost' i vnutrennyuyu nakoplennuyu energiyu metalla [Fatigue deterioration influence on hardness and internal accumulated energy]. *Vestnik Ufimskogo gosudarstvennogo aviatsionnogo tekhnicheskogo universiteta = Vestnik USATU*, 2007, vol. 9, no. 6 (24), pp. 152–157.

18. Aleshin N.P., Shcherbinskii V.G. *Radiatsionnaya, ul'trozvukovaya i magnitnaya defektoskopiya metalloizdelii* [Radiation, ultrasonic and magnetic flaw detection of metal products]. Moscow, Vysshaya shkola Publ., 1991. 271 p. ISBN 5-06-000923-8.

19. Gorkunov E.S., Savrai R.A., Makarov A.V., Zadvorkin S.M. Magnetic techniques for estimating elastic and plastic strains in steels under cyclic loading. *Diagnostics, Resource and Mechanics of Materials and Structures*, 2015, iss. 2, pp. 6–15. DOI: 10.17804/2410-9908.2015.2.006-015. (In Russian).

20. Makhutov N.A., Dubov A.A., Denisov A.S. Issledovanie staticheskikh i tsiklicheskikh deformatsii s ispol'zovaniem metoda magnitnoi pamyati metalla [Study of static and cyclic deformations using the metal magnetic memory method]. *Zavodskaya laboratoriya. Diagnostika materialov = Industrial laboratory. Materials diagnostics*, 2008, vol. 74, no. 3, pp. 42–46. (In Russian).

21. Muratov K.R., Novikov V.F., Neradovskii D.F., Kazakov R.K. Magnetoelastic demagnetization of steel under cyclic loading. *The Physics of Metals and Metallography*, 2018, vol. 119, no. 1, pp. 18–25. DOI: 10.1134/S0031918X1801012X. Translated from *Fizika metallov i metallovedenie*, 2018, vol. 119, no. 1, pp. 19–25. DOI: 10.7868/S0015323018010035.

22. Panin V.E., Panin A.V., Elsukova T.F., Kuzina O.Yu. Effekt "shakhmatnoi doski" v raspredelenii napryazhenii i deformatsii na interfeisakh v nagruzhennom tverdom tele: eksperimental'naya verifikatsiya i mekhanizmy mezoskopicheskogo kanalirovaniya [Effect of "chessboard" stress and strain distribution on interfaces in a loaded solid: experimental verification and mesoscopic channeling mechanisms]. *Fizicheskaya mezomekhanika = Physical Mesomechanics*, 2005, vol. 8, no. 6, pp. 97–105. (In Russian).

23. Kapustin V.I., Gileta V.P., Zakharchenko K.V. Eksperimental'noe izuchenie zakonomernostei deformirovaniya alyuminievykh splavov pri regulyarnykh nagruzheniyakh [The experimental study of regularities of aluminum alloys deformation in case of regular stresses]. *Obrabotka metallov (tekhnologiya, oborudovanie, instrumenty) = Metal Working and Material Science*, 2011, no. 4 (53), pp. 40–43.

24. Shanyavskii A.A., Banov M.D., Beklemishev N.N. *Diagnostika ustalosti aviatsionnykh konstruktsii akusticheskoi emissiei* [Diagnostics of fatigue of aircraft structures by acoustic emission]. Moscow, MAI Publ., 2017. 186 p. ISBN 978-5-4316-0405-8.

25. Kapustin V.I., Zakharchenko K.V. On the experimental analysis of dissipative processes under cyclic loading of metals. *Journal of Physics: Conference Series*, 2017, vol. 894, no. 1, p. 012128. DOI: 10.1088/1742-6596/894/1/012128.

26. Zakharchenko K., Kapustin V., Legan M., Larichkin A., Lukianov Y., Zverkov I. On the effect of plasma electrolytic oxidation on the fatigue strength of V96TS1 (Al-Zn-Mg-Cu) aluminum alloy. *Journal of Physics. Conference Series*, 2020, vol. 1666, no. 1, p. 012019. DOI: 10.1088/1742-6596/1666/1/012019.

27. Zakharchenko K.V., Kapustin V.I., Shutov A.V. On the analysis of energy dissipation and ratcheting during cyclic deformation of the titanium alloy VT6 (Ti-6Al-4V). *Journal of Physics. Conference Series*, 2020, vol. 1666, no. 1, p. 012025. DOI: 10.1088/1742-6596/1431/1/012025.

28. Diaz F.A., Patterson E.A., Tomlinson R.A., Yates J.R. Measuring stress intensity factors during fatigue crack growth using thermoelasticity. *Fatigue and Fracture of Engineering Materials and Structures*, 2004, vol. 27, no. 7, pp. 571–583. DOI: 10.1111/j.1460-2695.2004.00782.x.

29. Ranc N., Palin-Luc T., Paris P.C., Saintier N. About the effect of plastic dissipation in heat at the crack tip on the stress intensity factor under cyclic loading. *International Journal of Fatigue*, 2014, vol. 58, pp. 56–65. DOI: 10.1016/j.ijfatigue.2013.04.012.

30. Meneghetti G., Ricotta M. Evaluating the heat energy dissipated in a small volume surrounding the tip of a fatigue crack. *International Journal of Fatigue*, 2016, vol. 92, pt. 2, pp. 605–615. DOI: 10.1016/j.ijfatigue.2016.04.001.

31. Fridlyander I.N. Sovremennye alyuminievye, magnievye splavy i kompozitsionnye materialy na ikh osnove [Modern aluminum, magnesium alloys and composite materials based on them]. *Metallovedenie i termicheskaya obrabotka metallov = Metal Science and Heat Treatment*, 2002, no. 7, pp. 24–29. (In Russian).

32. Zakharchenko K.V., Kapustin V.I., Larichkin A.Yu. O vliyanii keramicheskogo pokrytiya na deformatsionnye kharakteristiki alyuminievogo splava D16AT [About the influence of ceramic coatings on the stress-strain characteristics of the alloy Д16АТ (Al-Cu-Mg)]. *Obrabotka metallov (tekhnologiya, oborudovanie, instrumenty) = Metal Working and Material Science*, 2014, no. 3 (64), pp. 37–44.

Conflicts of Interest

The authors declare no conflict of interest.